JOURNAL OF NANO- AND ELECTRONIC PHYSICS
Vol. 12 No 3, 03036(5pp) (2020)

ЖУРНАЛ НАНО- ТА ЕЛЕКТРОННОЇ ФІЗИКИ
Том 12 № 3, 03036(5cc) (2020)

Model of Tunneling Current on Bilayer Armchair Graphene Nanoribbon Tunnel Field Effect Transistor Using Transfer Matrix Method

E. Suhendi*, M.F. Fadhillah, I. Anjaningsih, S.D. Ulhaq, A. Fadhillah, D. Rusdiana

Program Studi Fisika, Universitas Pendidikan Indonesia, Bandung, Indonesia

(Received 27 September 2019; revised manuscript received 15 June 2020; published online 25 June 2020)

A tunneling current in bilayer armchair graphene nanoribbon (BAGNR) based tunnel field-effect transistors is modeled by semi-numeric methods. Potential profiles of field-effect transistors are divided into several segments by numerical methods. The Transfer Matrix Method (TMM) is a numerical method used in calculating electron transmittance values. The TMM method was applied to get the electron transmittance values, then the Landauer formula with the Gauss Legendre Quadrature (GLQ) method was applied to generate the tunneling current from TFETs. The tunneling current is calculated by changing a number of variables, namely gate voltage (V_G), drainage voltage (V_D), temperature, N index, the thickness of the oxide layer and device length. In this study, the calculation of the cut-off frequency on the tunneling field-effect transistor was also carried out. The results of the tunneling current calculation show that the greater value of V_G can affect the saturation current. The results of the tunneling current calculation show that the higher the temperature, the lower the tunneling current value. The calculation of the tunneling current also shows that the wider the BAGNR, the greater the tunneling current. This is due to the influence of BAGNR width which makes the energy gap (E_g) lower. The value of the cut-off frequency on the BAGNR tunnel field-effect transistor recorded in this study is 3.96-8.9 THz.

Keywords: Tunneling current, Tunnel field effect transistor, BAGNR, MMT, Cut-off frequency.

DOI: 10.21272/jnep.12(3).03036 PACS numbers: 81.05.Zx, 85.30.Tv

1. INTRODUCTION

Today, the electronic world has shown significant development. One of the interesting electronic components is transistors. These devices are commonly used as amplifiers, electronic switches, and components of the integrated circuits. In its development, transistors experience several obstacles such as thermionic effects and constraints of low energy use to reduce power dissipation. Based on some of these constraints, the transistor development was carried out in several aspects including the working mechanism, transistor design and transistor-making material [1]. One type of transistors that shows development is a field-effect transistor. A field-effect transistor (FET) is a transistor using an electric field to control a channel from a type of charge carrier in the semiconductor material. The development of FETs includes metal-oxide-semiconductor field-effect transistors (MOSFETs) and tunnel field-effect transistors (TFETs). The difference between a MOSFET and TFET lies in the transfer mechanism. The transfer mechanism in the MOSFET uses thermionic emissions that require a certain amount of energy so that the transistor can reach ON conditions while TFET uses a quantum tunneling mechanism [2]. A TFET is one of the electronic devices that shows a promising future. TFET has the advantage of exploiting low energy, a tunneling mechanism between bands that can reduce current leakage and fabrication similar to MOSFETs. With these advantages compared to MOSFETs, TFET is an alternative electronic device. TFET has the potential to be applied to devices that work with low energy and high frequency and energy efficiency which can be applied to integrated circuits [3].

Most of the materials used in electronic components are dominated by silicon. At present, the development of silicon as a semiconductor material is close to its limits. With the mobility of electrons below 1400 cm²/Vs, energy bands around 1.1 eV and decreasing performance at high temperatures provide opportunities for other solid materials to replace silicon as the basic material of electronic devices [4]. One alternative material that attracts the attention of researchers and continues to show progress is graphene. Graphene has superior characteristics than silicon including electron mobility of 200,000 cm²/Vs and energy bandgap at 0.5 eV [5]. The electronic properties of graphene show a variety of advantages that can make it an alternative to electronic basic materials. Based on its structure graphene can be divided into graphene monolayer, graphene bilayer, and multilayer graphene. Graphene bilayers with double stack structures have advantages in better structure, higher electric charge mobility and flexibility than graphene monolayer [6].

Several studies have investigated the ability of graphene in electronic devices given the characteristics of the electric current-potential FET from BAGNR [7], and simulation of tunneling currents on TFET device nanoribbon device transistors. It has been shown that the electron transmittance values with the airy function are calculated using several device parameters. The transmittance value obtained is then used to calculate the tunneling current. The results obtained show that current characteristics are similar to the characteristics of current MOSFETs in general.

In this study, we will calculate the tunneling current in tunnel field-effect transistor bilayer armchair graphene nanoribbon (TFET-BAGNR) using the

* endis@upi.edu

 © 2020 Sumy State University

transfer matrix method (TMM). The TMM can reduce calculation errors in numerical calculations and has been widely used in quantum phenomena [8]. The TMM is used to calculate electron transmittance, and the transmittance is used to calculate the tunneling current using a Landauer equation. Then it will be examined the effect of several parameters such as *N*-index BAGNR, temperature, and oxide layer thickness on the tunneling current in TFET. In addition to calculating the tunneling current, in this study, the calculation of the cut-off frequency in the TFET was calculated.

2. THEORETICAL MODELS

This paper reports on a study which calculates tunneling current in a graphene bilayer TFET using the TMM. The potential profile used in this study is based on the potential profile in the reference [7]. The solution of the Schrodinger equation in this calculation is done by applying the boundary conditions for each segment to get the transmittance value using the TMM already done. After the transmittance value is obtained, this value is used to calculate the tunneling current in TFET using the Landauer formula [9].

The tunneling current is dependent on the large probability of the electrons breaking through the potential barrier. Related tunneling currents in FETs can be formulated as follows [10]:

$$I = \frac{2qg_v}{\pi k\hbar} \int_{E1}^{E2} T(E)[f_S(E) - f_D(E)]dE, \qquad (2.1)$$

where $f_S(E)$ and $f_D(E)$ are the Fermi-Dirac distribution functions of the source and drain, respectively, h is the Planck constant, k_B is the Boltzmann constant, $T(E)$ is the transmission coefficient, and g_v is the GNR degeneration ($g_v = 1$).

The cut-off frequency is one of the important parameters that can represent the performance of an electronic device. The cut-off frequency can also be considered as the first thing that can be defined for frequency response because of an increase in the cut-off frequency that can reduce the intrinsic delay in the transistor. The cut-off frequency can be defined as follows [11]:

$$f_t = \frac{g_m}{2\pi C_g}, \qquad (2.2)$$

where g_m is the transconductance and C_g is the total capacitance at the gate. Transconductance can be defined as the first differential of the breakthrough current against the gate voltage as follows [11]:

$$g_m = \frac{\partial I_D}{\partial V_G}. \qquad (2.3)$$

3. RESULTS AND DISCUSSION

In this research, the tunneling current on TFET-BAGNR was simulated. This aims to determine the relationship between several variables and the tunneling current in the TFET.

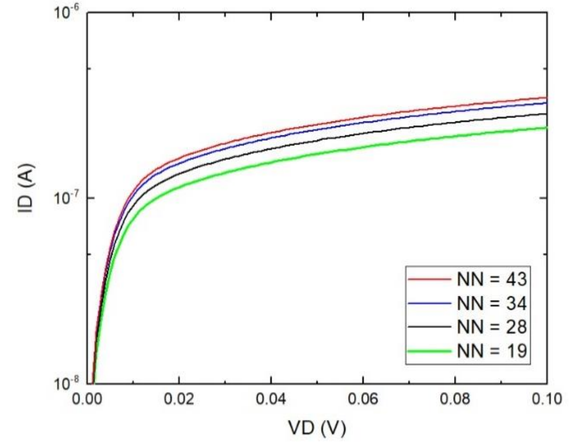

a

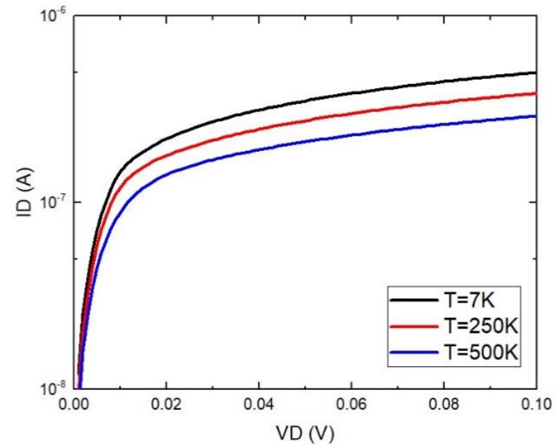

b

Fig. 1 – Tunneling current as a function of drain voltage (V_D) with variations of *N*-index (a); tunneling current as a function of drain voltage (V_D) with variations of temperature (b)

Fig. 1a shows the effect of *N*-index on the tunneling current on the TFET by comparing the value of the tunneling current at point $V_D = 0.1$ V. It can be observed that the value of the tunneling current is higher with increasing *N*-index of BAGNR. *N*-index of graphene affects the edges of BAGNR structure which form the width of BAGNR. The width of BAGNR has an effect on the bandgap energy (E_g) in graphene. In accordance with the present results, previous studies have shown that current density increases with increasing width of BAGNR and reaches a maximum when the width of the BAGNR reaches $\omega_0 = 6.5$ nm [12]. It is apparent from Fig. 1a that a relationship between the value of E_g with the *N*-index is inversely proportional. This result agrees with the findings of other studies in which it is shown that the BAGNR bandgap energy (E_g) decreases with increasing width of BAGNR [10, 12]. When the width of BAGNR increases, the bandgap energy decreases because one of conditions for tunneling process to occur in TFET. The difference in E_g values can affect a large number of electrons that can break through the barrier. Amount of tunneling current is due to the influence of the bandgap energy value on the semiconductor. This value can determine the minimum energy needed for

electrons in the semiconductor so that they can move from the valence band to the conduction band and then become the carrier charge on the transistor. This finding indicated that an increase in the width of BAGNR causes a decrease in the energy bandgap. Then the electrons more easily enter the conduction band and the holes are easier to enter the valence band. As a result, the tunneling current in the transistor is getting higher [10, 13].

As shown in Fig. 1b, the tunneling current value at point $V_D = 0.1$ V on the TFET can be affected by the temperature of the transistor. The data shows that the higher the value of the temperature, the lower the value of the tunneling current in the transistor. It shows an indication that the tunneling current is influenced by the temperature of testing. The temperature of testing in this study can affect thermal resistivity in semiconductor materials. A lower tunneling current when the temperature is higher because the thermal resistivity at high temperatures is higher than the low temperature. The high thermal resistivity can inhibit the rate of electrons to flow [14]. Further analysis shows that another cause of decreasing tunneling current influenced by increasing temperature is the carrying charge of graphene affected by temperature. This is due to the collision mechanism that occurs in graphene, namely the phonon collision. The effect of the phonon collision with the carrier charge in both graphene monolayer and graphene bilayer is very weak in the temperature range 0-300 K. In graphene bilayer, the effect of phonon scattering is smaller than that occurring in graphene monolayer. Therefore, bilayer graphene has a stable level of carrier charge mobility in this temperature range. Based on previous experiments at temperatures of 273-513 K, an indication of the temperature has little effect on the mobility of graphene bilayer load carriers. This is because the main scattering source does not have a significant effect on the load carrier conditions in graphene [15].

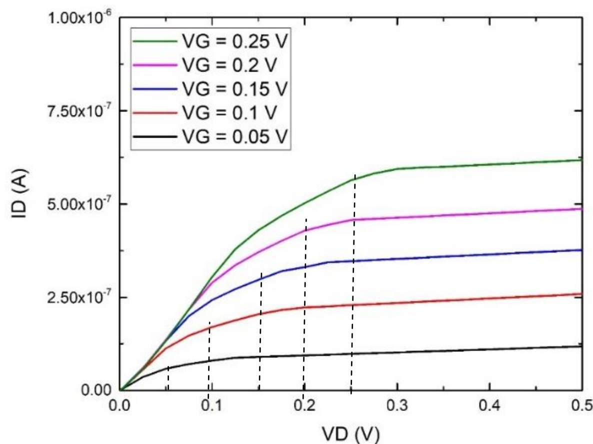

Fig. 2 – Tunneling current as a function of drain voltage (V_D) with variations of gate voltage (V_G)

Fig. 2 shows that the tunneling current, which is higher than the V_D value from 0-0.1 V, increases the tunneling current value proportional to the increase in V_D value. To find out the effect of the gate voltage on the transistor, it can be seen based on the current value at point $V_D = 0.1$ V. It can be seen in Fig. 2 that the higher gate voltage value (V_G), the bigger the tunneling current produced. This happens based on the working principle of a FET that is affected by voltage. When the drain voltage V_D gets bigger, the channel area will be thickened so that the channel narrows and the barrier on the channel gets bigger. According to this result, it can be found that the relationship between conductor resistance and cross-sectional area is inversely proportional. For larger V_D, the emptying area will get bigger and close the channel. This causes clamping on the channel and the current undergoes saturation, and V_D voltage where this occurs is called pinch voltage (V_P) [16]. The value of the tunneling current in the range $V_D > 0.2$ V is no longer experiencing a significant increase, this can be affected by pinch voltage (V_P). Tunneling current at $V_D > 0.2$ V reaches saturation conditions. Saturation conditions occur when the edge of the conduction band on the channel is lower than the channel, where the conduction band edge is dependent on gate voltage [17]. The gate voltage on the device affects the value of the pinch voltage that occurs on the device. The pinch voltage on the device can make the tunneling current undergoes saturation conditions which mean that there is no increase in the flow of electrons that break through the barrier. Based on Fig. 2 the saturation current in TFET corresponds to the saturation conditions in conventional FET [10].

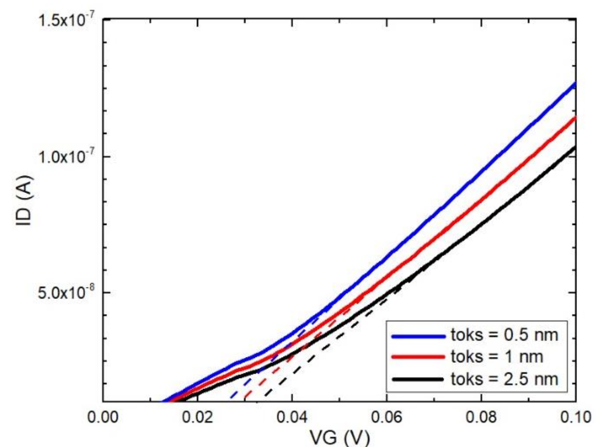

Fig. 3 – Tunneling current as a function of gate voltage (V_G) with variations of oxide layer thickness

Fig. 3 shows the calculation results of the tunneling current against the gate voltage variations for several layer thickness variables. Based on this figure, the tunneling current is recorded at $V_G > 0.01$ and continues to rise in proportion to the increase in V_G. The current that has not occurred at $V_G < 0.01$ can be caused by a channel that has not been formed so that the electrons in the source area have not been able to flow to the drain area. The most interesting of this graph is decreasing current value based on the increasing thickness oxide layer at the gate. It is shown in Fig. 3, that when the current at the gate voltage $V_G = 0.1$ V, the tunneling current value is inversely proportional to the thickness of the oxide layer at the transistor gate. But the difference in current values is not too high compared to the current for the thickness of the other

oxide layers. This can indicate that the thicker the oxide layer in the transistor, the lower the current produced by the transistor. This phenomenon can be influenced by the charge capacitance at the gate which is getting higher when the thickness of the oxide layer is getting lower. The charge capacitance at the gate can make it easier for electrons to flow from the gate to the channel so that the tunneling current gets bigger [18]. The effect of oxide layer thickness on tunneling current has characteristics similar to MOSFETs and CNT-FETs [7]. Further analysis of the data reveals that the thickness of the oxide layer can affect the threshold voltage value (V_{TH}). The threshold voltage is the minimum voltage value at the gate-source that is needed so that the carrier charge can flow from the source to the channel [11]. The threshold voltage (V_{TH}) can be shown by a dashed line in Fig. 3 at point $I_D = 0$ A. The significant difference in the value of the threshold voltage is due to the difference in thickness of the oxide layer. This result shows that the threshold voltage value in the transistor is getting higher along with the thickness of the oxide layer. This means that a higher voltage value is needed so that the carrier load can flow to the drain.

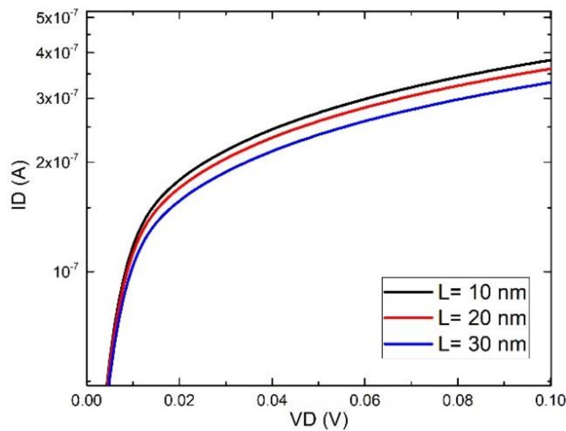

Fig. 4 – Tunneling current as a function of drain voltage (V_D) with variations of channel length

Fig. 4 shows the tunneling current in the transistor against changes in drain voltage (V_D). The tunneling current has a significant increase in the drain voltage range $V_D < 0.01$. When $V_D > 0.01$ the tunneling current begins to a saturation phase. This is indicated by an increase in current that is not significant and tends to be stable. This saturation condition is caused by the drain voltage that has closed the channel. With the closure of the channel, the tunneling current is no longer increasing. Based on the above graph, the tunneling current value is obtained at point $V_D = 0.1$ V. The tunneling current value of the transistor at that point has different values for different device lengths. Based on this data, the tunneling current value has decreased along with the length increase in the transistor channel. The influence of device length on the tunneling current in the TFET can be influenced by the resistivity value. For large devices, the resistivity value will be greater so that the tunneling current that occurs will be smaller. It is inversely proportional to the smaller device length. The resistivity value will be greater so that the tunneling current will be greater [19].

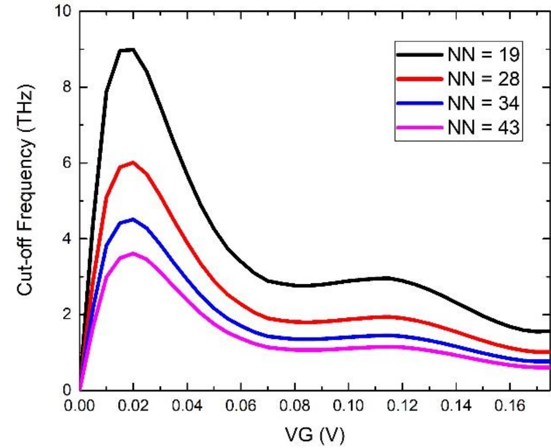

Fig. 5 – Cut-off frequency as a function of gate voltage (V_G) with variations of *N*-index

In this study, a simulation was performed on the calculation of the cut-off frequency for TFETs. The cut-off frequency is one of the characteristics of a transistor. It is the frequency that exceeds or less than the operating range, and it may cause the transistor fails to operate. Based on the picture above, the calculation model for the cut-off frequency for TFETs with several predetermined calculation parameters is obtained. The frequency value in the TFET increases at $V_G = 0$-0.02 V to the maximum frequency. This can occur because of an increase in transconductance and a decrease in the total gate capacitance value (*Cg*) at the gate. However, the cut-off frequency in this simulation has decreased for $V_G > V_{TH}$. This happens because there is an increase in the total capacitance of the gate in the condition ON. Higher *Cg* in TFETs is caused by the capacity at the gate to the dominant drain because the presence of a large breakthrough barrier between the channel and the source in the ON state can reduce the effect of gate capacitance and source. The capacitance value at the gate will rise as the gate voltage reaches the saturation condition [18]. The cut-off frequency value shown in this simulation has a better value than the cut-off frequency value indicated by a conventional graphene MOSFET experiment that has a value of 800-1400 GHz. The difference in the cut-off frequency value in this study is because the modeling carried out assumes that the transport that occurs is ballistic transport and ignores the interface effect in the simulation [20].

4. CONCLUSIONS

In this research, a tunneling current calculation in TFET-BAGNR using TMM was performed to obtain electron transmittance. Electron transmittance is then used to calculate the tunneling current with the Gauss-Legendre quadrature method. The tunneling current in the transistor is influenced by the bandwidth of BAGNR, the thickness of the oxide layer at the gate, *N*-index of BAGNR, temperature and device length. The cut-off frequency is one of the important parameters in reviewing the performance of transistors and the cut-off frequency value recorded in this study is 3.5-8.9 THz.

ACKNOWLEDGEMENTS

This work was financially supported by "Hibah Penelitian Berbasis Kompetensi" Research Grants in the fiscal year 2019, KEMENRISTEKDIKTI Republic of Indonesia.

REFERENCES

1. S.-G. Zang, X.-Y. Liu, X. Lin, L. Liu, W. Liu, D.W. Zhang, P.-F. Wang, W. Hansch, *IEEE Int. Conf. Solid-State Integ. Circuit Technol.,* 1238 (2010).
2. U.E. Avci, D.H. Morris, I.A. Young, *J. Electron Devices Soc.* **3** No 3, 88 (2015).
3. M. Aswathy, N.M. Biju, R. Komaragiri, *Int. Conf. Adv. Comput. Communic. (ICACCI'13),* 149 (2013).
4. S.M. Sze, *Physics of Semiconductor Devices* (New York: John Wiley: 1981).
5. H. Raza, *Graphene Nanoelectronics; Metrology, Synthesis, Properties, and Applications* (New York: Springer-Verlag: 2012).
6. H. Yan, *Nanophotonics* **4** No 1, 115 (2015).
7. E. Sustini, R. Syariati, *J. Phys. Conf. Ser* **1120** No 1 012095 (2018).
8. C. Jirauschek, *IEEE J. Quantum Electron* **45** No 9, 1059 (2009).
9. C.S.P. Bimo, F.A. Noor, M. Abdullah, Khairurrijal, *Adv. Mater. Res.* **896**, 371 (2014).
10. E. Suhendi, L. Hasanah, D. Rusdiana, F.A. Noor, N. Kurniasih, *J. Semicond.* **40** No 6, 062002 (2019).
11. P. Kumari, S. Dash, G.P. Mishra, *Adv. Nat. Sci.-Nanosci.* **6** No 4, 045005 (2015).
12. D. Jena, T. Fang, Q. Zhang, H. Xing, *Appl. Phys. Lett.* **93**, No 11, 112106 (2008).
13. E. Suhendi, F.A. Noor, N. Kurniasih, *Adv. Mater. Res.* **896**, 367 (2014).
14. E. Suhendi, R. Syariati, F.A. Noor, N. Kurniasih, Khairurrijal, *AIP Conf. Proc.* **1589** No 1, 91 (2014).
15. S.V. Morozov, K.S. Novoselov, M.I. Katsnelson, F. Schedin, D.C. Elias, J.A. Jaszczak, A.K. Geim, *Phys. Rev. Lett.* **100** No 1, 016602 (2008).
16. Sutrisno, *Elektronika: Teori dan Penerapannya 1* (Bandung: Penerbit ITB: 1986).
17. E. Suhendi, F.A. Noor, N. Kurniasih, *Adv. Mater. Res.* **974**, 205 (2014).
18. K.P. Pradhan, S.K. Mohapatra, P.K. Sahu, D.K. Behera, *Microelectron. J.* **45** No 2, 144 (2014).
19. B. Bhowmick, S. Baishya, J. Sen, *Electron. Lett.* **49** No 16, 1031 (2013).
20. B. Rawat, R. Paily, *IEEE T. Electron Dev.* **62** No 8 2663 (2015).

Модель тунельного струму у тунельному польовому транзисторі на базі двошарової графенової нанострічки за допомогою методу матриці переносу

E. Suhendi, M.F. Fadhillah, I. Anjaningsih, S.D. Ulhaq, A. Fadhillah, D. Rusdiana

Program Studi Fisika, Universitas Pendidikan Indonesia, Bandung, Indonesia

Тунельний струм в тунельних польових транзисторах на базі двошарової графенової нанострічки (BAGNR) моделюється напівчисловими методами. Потенційні профілі польових транзисторів діляться на кілька сегментів за числовими методами. Метод матриці переносу (ТММ) – це числовий метод, що використовується для обчислення коефіцієнта проходження електронів. Використовуючи результати обчислення коефіцієнта проходження електронів методом ММТ, тунельний струм був отриманий за формулою Ландауера за допомогою методу квадратур Гауса-Лежандра. Тунельний струм обчислюється варіацією числа змінних, а саме напруги затвору (V_G), напруги стоку (V_D), температури, коефіцієнту N, товщини оксидного шару та довжини пристрою. У цьому дослідженні також був проведений розрахунок частоти зрізу на тунельному польовому транзисторі. Результати розрахунку тунельного струму показують, що більше значення V_G може впливати на струм насичення. Крім того, чим вища температура, тим нижче значення тунельного струму. Розрахунок тунельного струму також показує, що чим ширше BAGNR, тим більший тунельний струм. Це пов'язано з впливом ширини BAGNR, що робить ширину забороненої зони (E_g) меншою. Значення частоти зрізу на тунельному польовому транзисторі на базі BAGNR, отримане в цьому дослідженні, становить 3,96-8,9 ТГц.

Ключові слова: Тунельний струм, Тунельний польовий транзистор, BAGNR, ММТ, Частота зрізу.